*Proceedings of the 10th International Conference on Heat Transfer and Fluid Flow (HTFF 2023)*
*Brunel University, London, United Kingdom –August 06-08, 2023*
*Paper No. HTFF 150*
*DOI: 10.11159/htff23.150*

# Unsteady Wake And Dynamic Characteristics Of Flow Past Two Inline Circular Cylinders

**Shristi singh[1], Shaligram Tiwari[2]**
Indian Institute of Technology Madras
Chennai-600036, India
[1]shristithakur995@gmail.com; [2]shaligt@iitm.ac.in

***Abstract –*** Open-Source Field Operation and Manipulation (OpenFOAM 7) software, has been used for a two- dimensional (2D) numerical computations, to study unsteady wake characteristics in flow past two inline stationary circular cylinders. The solver (icoFoam) employs a finite volume based method (FVM) for discretization and computations. Computations are executed for the range of Reynolds number (Re) from 100 to 250 and for the range of inter-cylinder spacing (S) from 2 to 5. Effects of S and Re on the wake flow behaviour and dynamic coefficients for the cylinders have been presented. Four different values of S and Re have been considered which show influence on both the wakes, with stronger effect on the wake behind the downstream cylinder. To analyse unsteady wake characteristic, the time series of transverse velocity component has been used. In addition, the lift signals of both the cylinders have been analysed to study the phase dependence on S and Re.

***Keywords:*** *Two inline circular cylinders; vortex shedding; strouhal number; drag and lift, fluctuation of lift coefficient*

## 1. Introduction

It is well known that if there is any change in Reynolds number (Re), the wake of single circular cylinder undergoes various transitions. Initially, when the Re is very low (<10), flow is laminar and steady and there is no any separation from the cylinder surface. As Re increases from 10 to 50, flow is remains laminar and steady, but separation occurs from lateral surface in form of two symmetric vortex bubbles behind the cylinder [1]. With further increase in Re, there is onset of the vortex shedding that takes place alternatively from lateral surfaces of the cylinder, being described as one of the important type of bifurcation named as Hopf bifurcation. However, multiple bodies are there in a fluid flow, the resulting flow field and fluid forces differ from those observed when a isolated body is present in the same fluid flow. This phenomenon, known as wake interference, is commonly noticed in various engineering applications, such as piers, bridge, offshore platforms and heat exchangers. To study wake interference there is one ideal model which is flow past cylinders placed in tandem arrangement. This kind of flow has been extensively studied through both experimental and computational means due to its significant relevance [2]. The focus of early studies in the tandem systems is to find out the mechanical characteristics of the structural components. Later, the researchers shifted their interest to study the various flow regimes according to the value of Re and the separation of the two cylinders [3]. The hydrodynamic force behaviour and wake topology are analysed for each flow regime. While there were differences in the level of detail in the classifications, it is generally agreed upon that as the L/D changes, there are two distinct flow regimes: one is reattachment regime and another one is co-shedding regime [4]. According to the literature, in a reattachment regime shear layers from upstream cylinder reattach to the surface to the downstream cylinder and drag experience by the downstream cylinder remain negative in this regime. On the other hand, vortex shedding takes place behind each cylinders, drag becomes positive in co-shedding regime. Thus, to determine flow transition, critical spacing between cylinders plays an important role, as the sign of the downstream cylinder's drag changes based these spacing [5]. The separation between the regimes, which demarcates the critical spacing, is called to as drag inversion separation $[(L/D)_c]$ [6]. Moreover, subcritical to transcritical Re have been used for almost all the experiment done by the researcher on the flow past two tandem cylinders with similar diameters ($103\times10^5 \leq Re \geq 105\times10^5$) [7]. In this

range, various flow regimes are characterized that mainly depend on the spacing and less on the value of Re. Flow past the tandem cylinders with varying inter-cylinder spacing and different diameters has been studied by Wang et al. [8], for Re < 100. To investigate the initial stages of instability and the unstable modes in a steady flow and to examine the primary instability features, they conducted direct numerical simulations (DNS). Some of the researchers have shown interest in phase lag between two bodies. Alam et al. [9] carried out 2-D numerical simulations for Re = 200 and obtained the relation between phase lag and inter-cylinder spacing.

There is enough literature available on role of upstream cylinder, with varying size of the cylinders on the unsteady wake of the downstream cylinder with different values of inter-cylinder spacing. However, there is limited literature on the onset of unsteadiness and wakes interaction for both the cylinders. Detailed two-dimensional numerical simulation is conducted for different spacing and different values of Re to find out the wake characteristic and unsteadiness for both the cylinders. With the help of vorticity contours, the temporal wake behaviour and vortex-shedding mechanisms have been addressed. The relation between Cl, spacing (S) has been analysed to study the in-phase and out-phase cylinder between the wake of both the cylinder.

## 2. PROBLEM STATEMENT

Two-dimensional cartesian computation domain is shown in the figure below. A rectangular domain with the dimensions $L_1 = 40D$ and $L_2 = 16D$ is used, and two cylinders of same diameter are kept in that domain. Diameter (D) of the cylinder was selected as characteristic length scale and free stream velocity ($U_\infty$) was chosen as characteristic velocity scale. Non-dimensional inter-cylinder spacing becomes, S = s/D and variation of S is from 2 to 5, where s = dimensional spacing between centres of the two cylinders. To determine the unsteady wake characteristics, different values of S and Re have been chosen.

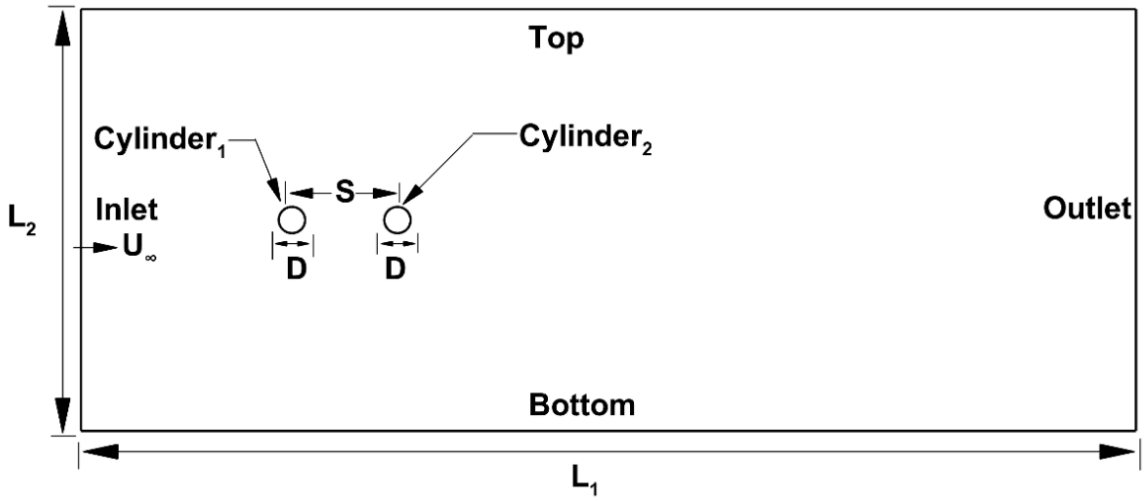


Fig. 1: Schematic diagram of the computational domain.

## 3. GOVERNING EQUATIONS AND BOUNDARY CONDITIONS

### 3.1. Governing Equations

Two dimensional (2-D) mass conservation equation and the momentum conservation equations have been solved for incompressible, unsteady and laminar flows. Following are the non-dimensionalized tensor forms of continuity equation and momentum equation.

$$\frac{\partial Ui}{\partial Xi} = 0 \qquad (1)$$

$$\frac{\partial Ui}{\partial t} + \frac{\partial (UiUj)}{\partial Xj} = -\frac{\partial P}{\partial Xj} + \frac{1}{Re}\frac{\partial^2 Ui}{\partial Xj \partial Xj} \quad (2)$$

Nondimensionalization is done for coordinate directions and velocity using characteristic length and characteristic velocity respectively. Here, Ui represents U velocity component and V velocity component in X direction and Y direction. The Reynolds number defined as

$$\mathrm{Re} = \frac{U_\infty D}{\nu} \quad (3)$$

Where D = diameter of either cylinder, $U_\infty$ = free stream velocity and ν = kinematic viscosity of the fluid.

### 3.2. Boundary Conditions

The given boundary conditions has been used for the computational domain at different boundaries as well as to the surfaces of the both the cylinders.

(i) Uniform velocity ($U = U_\infty$ and $V = 0$) at inlet.

(ii) Outlet Pressure ($P = 0$).

(iii) Symmetry condition ($V = 0$, $\frac{\partial U}{\partial Y} = 0$, $\frac{\partial P}{\partial Y} = 0$) at top and bottom surfaces.

(iv) No-slip and impermeability boundary conditions ($U = 0$ and $V = 0$) at cylinder surfaces.

## 4. GRID AND NUMERICAL TECHNIQUE

### 4.1. Grid Mesh and Grid Independence

To generate 2-D structured grid, ICEM-CFD 2021(commercial software) has been used. The refined grid is used near the circumference of the cylinder surface and grid size increased uniformly towards the outer region with a fixed ratio. The two inline circular cylinders of equal size for S =4 at Re = 100 is used for grid independence study. Four different arrangements of grid distribution on the circumference of both the cylinders is used to find out mean drag coefficient of both upstream cylinder and downstream cylinder, which is shown in below Table-1. It may be noticed that the case of 120 grid points does not give rise to significant change on further refinement. Consequently, the refinement corresponding to 120 grid points on circumference of each cylinder has been used for all the computations.

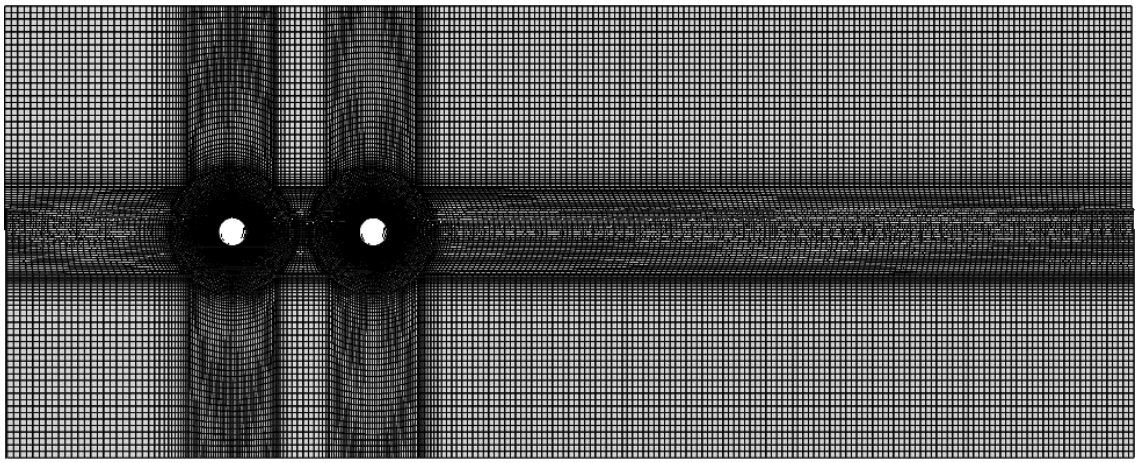

Fig. 2: Grid distribution around the cylinder.

### 4.2 Numerical Technique:

In two-dimensional flow, the Navier-Stokes equations have been solved using an ico foam solver (Open FOAM 7, C++ libraries) which is working on collocated grid system using the FVM (finite volume method). PISO (Pressure Implicit with the Splitting of Operators) algorithm has been used for velocity and pressure couplings. The discretization of convective and diffusive fluxes follows the Gauss linear scheme, while temporal

discretization is achieved using a 2nd order backward implicit scheme. Continuity equation and momentum equation have been assigned an absolute convergence criteria of $10^{-6}$.

Table-1: Grid independence result at Re = 100 for S = 4.

| Total number of grid points on the circumference of each cylinder | Upstream cylinder | | Downstream cylinder | |
|---|---|---|---|---|
| | $Cd_{mean1}$ | % change | $Cd_{mean2}$ | % change |
| 80 | 1.393 | - | 0.81 | - |
| 100 | 1.382 | 0.7396 | 0.799 | 1.358 |
| 120 | 1.375 | 0.5065 | 0.796 | 0.3754 |
| 160 | 1.373 | 0.1454 | 0.7940 | 0.2512 |

## 5. RESULTS AND DISCUSSION

### 5.1. Validation

For validation of computational work the case of single circular cylinder has been used to check accuracy of present work. This analysis has been done at a fixed Re (=100). Comparative analysis of St and Cd values has been done based on present work and literature by [10], [11]. After this comparison it has been noted that there is similarity in the results with the existing literatures and it presented in Table-2.

Table-2 Comparison of the values of $Cd_{mean}$ and St for the case of single stationary circular cylinder at Re = 100.

| Work/ study | Author(s) | $Cd_{mean}$ | St |
|---|---|---|---|
| Present work | - | 1.42 | 0.17 |
| Numerical | Mahir et al. (2008) | 1.368 | 0.172 |
| | Singha et al. (2010) | 1.431 | 0.165 |

### 5.2 Unsteady Wake Characteristics

Figure 2 represents vorticity contours for the case with flow past two inline circular cylinders. Figure 2(a) shows vorticity distribution for different-different value of S and fixed value of Re = 100. For small spacing ($S \leq 2$) between the cylinders, there is no vortex shedding behind downstream cylinder as there is wrapping of shear layers around the downstream cylinder which is coming from upstream cylinder. There downstream cylinder act as a splitter plate in wake of upstream cylinder, suppressing or preventing occurrence of the vortex shedding. As distance between the cylinders is increased, there is reattachment of the separating shear layers from the upstream to the downstream cylinder, and there is no independent vortex shedding is occurred in the wake of upstream cylinder. Even though shear layers grow behind upstream cylinder but presence of downstream cylinder, detachment of fully grown vortices is restricted. Moreover, as the distance between the cylinders is increased, separate periodic shedding of vortices is observed behind each of the cylinder. The unsteady behaviour of the upstream wake has been noted, but the presence of the downstream cylinder clear formation of karman vortex street prevents. Due to interaction of these vortices with shear layers of downstream cylinders, the vortex shedding becomes unsteady and irregular. Figure 2(b) presents vorticity contours for the S = 2 to 5 at Re = 150. At this Re, even when spacing is very less, there is periodic vortex shedding occur behind the downstream cylinder. When spacing is more ($S \geq 4$) some different type of pattern was found behind downstream cylinder. For such cases there is vortex shedding behind both cylinders and vortices detach from the upstream cylinder stretch the shear layer of the downstream cylinder and these vortices Has impact on vorticity pattern behind the downstream wake. In Figure

2(c), which shows vorticity contours at Re = 200 for S=2 to 5. The different spacing values, the shedding pattern looks similar to that observed at Re = 150, but the strength and frequency of the shed vorticity are different. In certain areas of the vorticity contours, there are more shed vortices, which suggests that the shedding frequency increases as the Reynolds number rises for a fixed value of S. In Figure 2(d), vorticity contour is shown for Re = 250 and S=2 to 5. At a Re of 200, a similar flow pattern can be noticed, although the strength and frequency are different for the shed vortices. When the Reynolds number is low, the wakes are more elongated behind the cylinder upstream than those observed at high Reynolds numbers, as demonstrated in Figure 2.

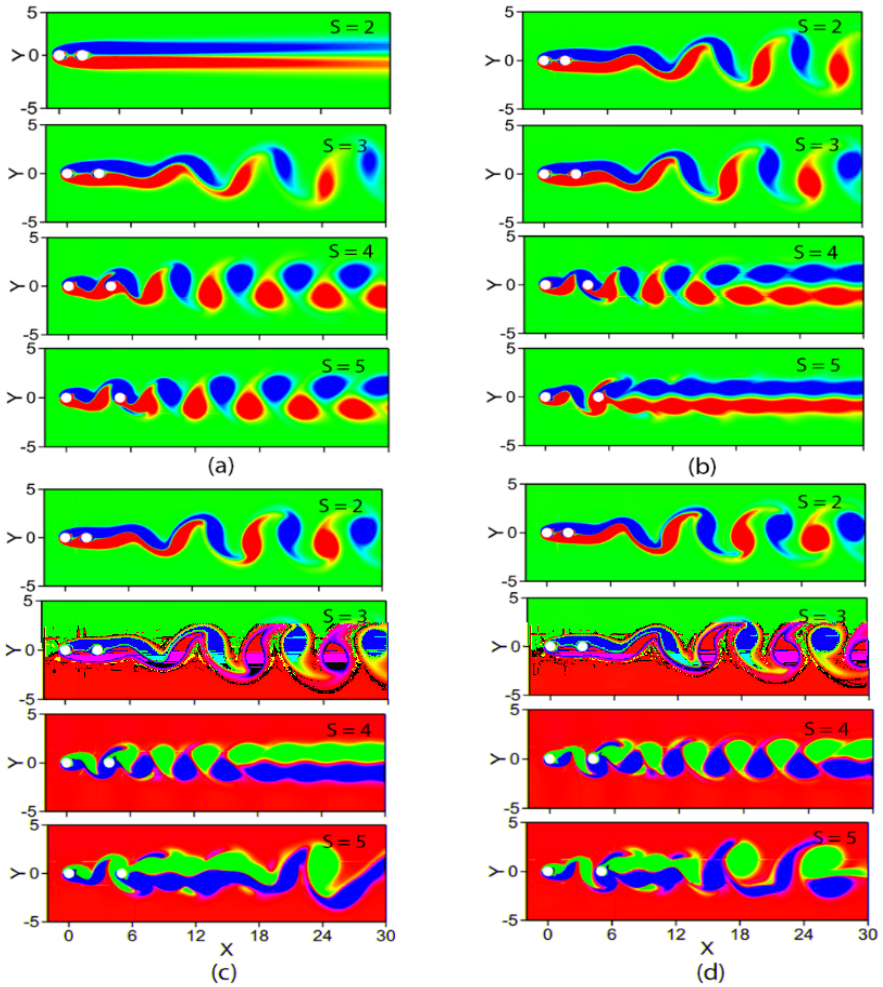


Fig. 2: Vorticity contours for different values of S (a) Re = 100, (b) Re = 150, (c) Re = 200 and (d) Re = 250.

The Figure 3 represents transverse velocity component of time signals in downstream wakes for different Re and S values over a time duration of 10 seconds. Additionally, RMS value of lift coefficient has been illustrated for each corresponding signal. Eddies are detached alternately from the cylinder surfaces, causing time-varying forces both stream wise and cross-flow. The characteristics of the unsteady wake are revealed by these forces, which have been analysed to understand wake behaviour. The amplitude of the signal reflects the nature of the wake; a minimal amplitude indicates a stationary or periodic signal, whereas unevenness in amplitude indicates non-linear interaction in a non-stationary signal. With the exception of Re = 100 and S = 2, the downstream wake is unsteady for each values of S and Re. Amplitude of the velocity signal increases with S, which indicate a higher level of wake unsteadiness. At low Re values, the signals seem to be of a harmonic type. However, at high Re values and corresponding to larger S values, fluctuations in amplitude can be observed. When the shedding occurs

in wakes at S = 4, the amplitude of signal is observed to be more in the downstream wake. With an increase in Re, there is a corresponding increase in the degree of unsteadiness and velocity signal's amplitude. This trend can be seen in the figure below, where a greater degree of unsteadiness and higher amplitude of velocity signals are seen at Re = 200 as compared to Re = 150, and similarly for Re = 250 as compared to Re = 200.

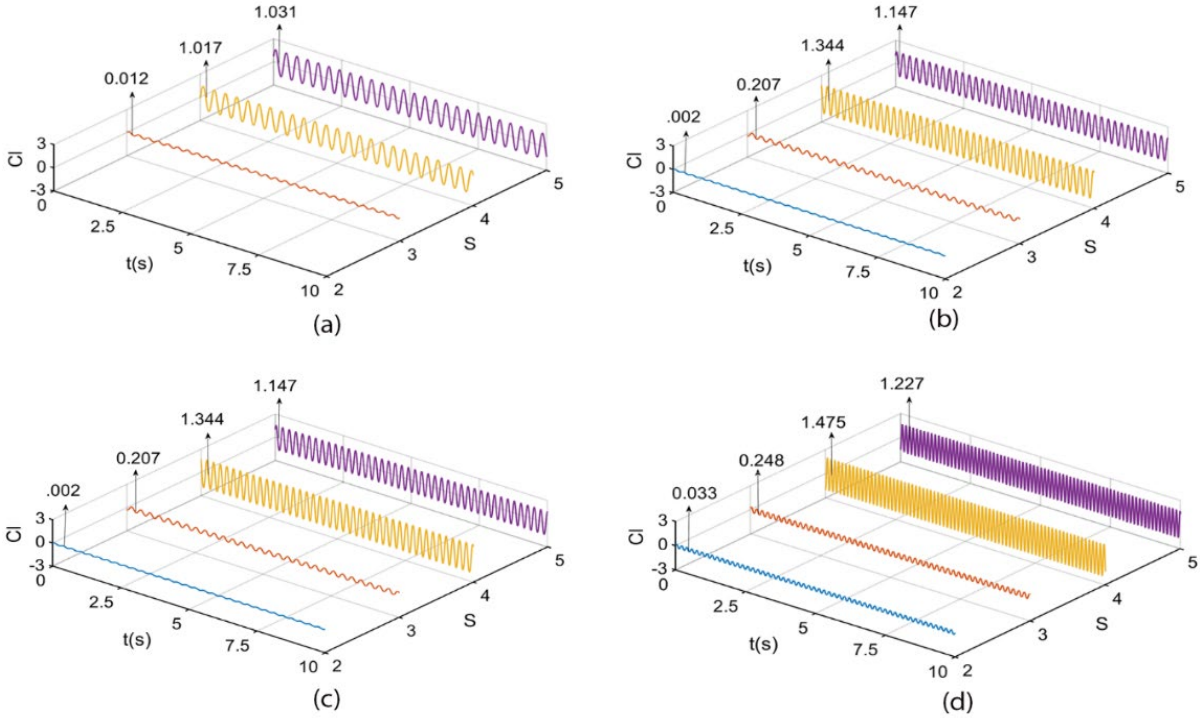


Fig. 3: Time series of Cl at different values of S for downstream cylinder (a) Re = 100, (b) Re = 150, (c) Re = 200 and (d) Re =250.

### 5.3 Dynamic characteristics

Figure. 4 represents, mean drag coefficients (Cd1 &Cd2) variations and the Strouhal number (St) in wake of the downstream cylinder, with S = 2 to 5 and Re = 100 to 250. The flow that impinges on downstream cylinder can be modified by adjusting S value between the cylinders. If the S value is small (L/D < 3), static pressure increases due to the presence of downstream cylinder (compared with static pressure of an isolated cylinder) behind the upstream cylinder. So that drag value of upstream cylinder decrease. For each value of Re, as S increases, drag value on upstream cylinder (Cd1) also increases monotonically. When the value of S increases, the size of the wake bubble behind the cylinder located upstream also increases. This leads to a higher-pressure drop-in wake, resulting in increase in form drag. Fig. 4 (b) represent a gradual increase in mean Cd2 of downstream cylinder for lower values of S, with a negative value observed across all Re values. This behaviour is attributed to presence of a low pressure region created by upstream cylinder, into which the downstream cylinder is immersed. While, when S is increased, the flow impinges with larger vortices on the upstream face of downstream cylinder, inducing to a corresponding rise in drag coefficient (Cd2). At higher Re values, a significant jump in the value of Cd2 is observed when S transitions from 3 to 4. This sudden increase can be attributed to shift of the flow pattern from reattachment mode to co-shedding mode [4]. The relationship between Strouhal number (St) and variations in S for different Re values is depicted in Fig. 4 (c). The St value has been derived from the Fourier spectra of time signal of lift coefficient for downstream cylinder. In fact, in the present work, lift signals for both the cylinders give same value of St for all the values of S and Re. It is noticed that the S has strong influence on St. The shedding frequency shows appreciable increase with increase S for all the values of Re. For given value of S, except S = 2, an increase

in Re does not show appreciable effect on change in St for S values less than or equal to 3. On the other hand, for higher S values, there is small increase in St with increase in the value of Re. When Re value is fixed and with increase in the value of S, the shedding of vortices coming from upstream cylinder reinforce shedding of vortices from downstream cylinder, causing vortex shedding frequency (St) to increase. The same value of St obtained for both the cylinders confirms that vortex shedding phenomena of both cylinders are highly correlated.

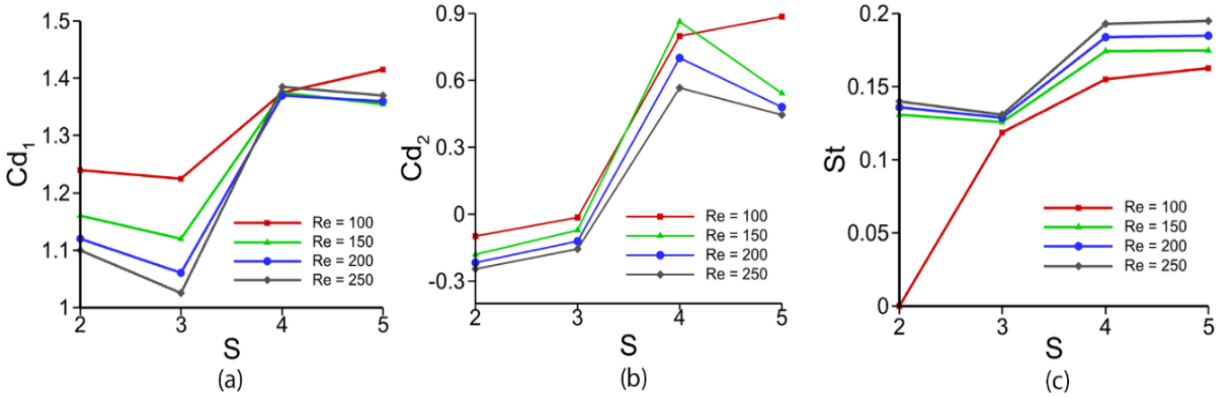


Fig. 4: Variation of (a) $Cd_1$ , (b) $Cd_2$ and (c) St, with spacing (S) for different values of Re.

### 5.4 Effect of S on Cl

Figure 5 represents the fluctuations of Cl signals for upstream cylinder and downstream cylinder for S = 2 to 5 and Re=100. When S increases, the mean parameters, St and Cd rise with increase in S as discussed earlier. While, fluctuating parameters, such as Cl, shows a wavy/ sinusoidal variation with S. For small value of S (S=2) both the signals are not totally out of phase but for S = 3, both the signals are out of phase for each value of Re. As spacing increases, lift signals are in phase for a fixed value of Re for both the cylinders. In the case of in-phase flow there is a growth of shear layer on both the cylinder surface simultaneously and vortex shedding occurs behind both the cylinder. There is a pull on the same side shear layer of the upstream cylinder which is exerted by shear layer of a downstream cylinder growing in a low pressure region. This results in an increase in velocity of shear layer of upstream cylinder and Cl attaining maximum value for in-phase flow. In the case of out-of-phase flow, there is a pull on the opposite side shear layer of upstream cylinder which is exerted by growing shear layer of the downstream cylinder where shear layers grow on opposite sides of the cylinders. As a result, the lift generated by the shear layer of upstream cylinder is reduced. This results in the value of Cl attaining minimum for the out-of-phase flow. For all values of Re, at S = 4, in-phase vortex shedding is found to occur. If S value is increase beyond 4, the lift signals for both the cylinders become out-of-phase again. This confirms that for fixed value of Re, the phase difference between lift signals of both the cylinders depends on inter-cylinder spacing.

## 6. Conclusion

The transitional wake behaviour of flow past on the two inline cylinders with varying spacing (S) and Reynolds number (Re) have been investigated through numerical computations. It is found that there is a delay of the transition in the wake due to presence of downstream cylinder behind upstream cylinder as compared to the case of flow past an isolated cylinder. Such a transition will depend on the inter cylinder spacing. Wake characteristics have been analysed with the help of vorticity contours. A transition from periodic to aperiodic nature is noticed in the wake, with increase in S and Re by analysing the time series signal of the lift coefficient of the downstream cylinder. The value of mean drag coefficient for the upstream cylinder increase with increase in the value of S and Re. Meanwhile, initially mean drag coefficient value increases and then decreases for the downstream cylinder. The St value increases with increase in Re and S. The lift signal is found to illustrate phase dependence with change in S and Re.

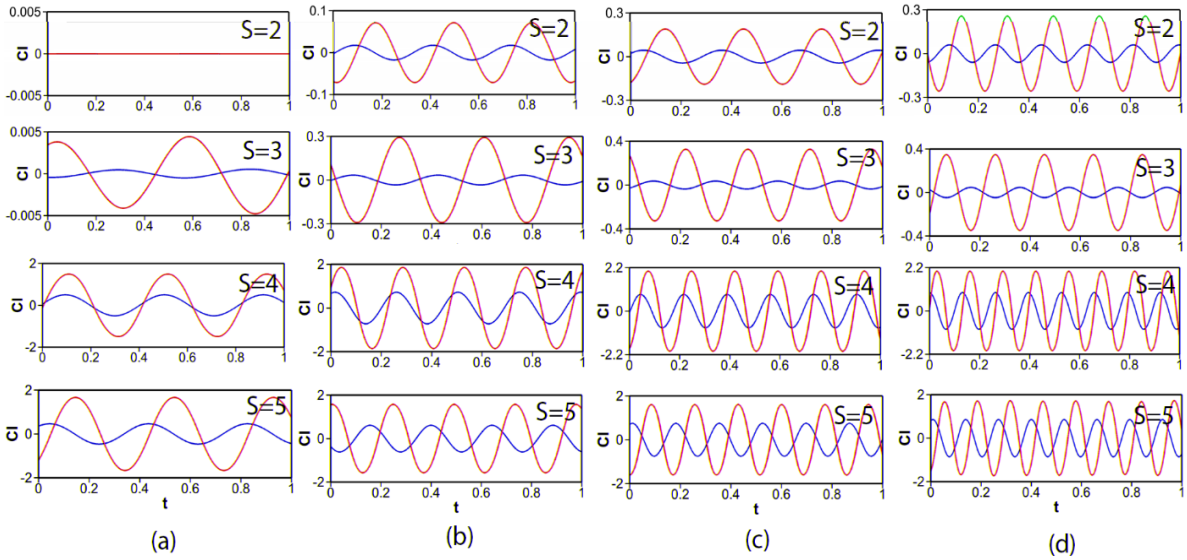


Fig. 5: Variation of Cl for both the cylinder (Red - upstream cylinder and green – downstream cylinder) at (a) Re =100, (b) Re = 150, (c) Re = 200 and (d) Re =250.

## Acknowledgements

Authors thank the High-Performance Computational Facility at IIT Madras, Chennai-600036, India.

## References

[1] A. Sohankar, C. Norberg, and L. Davidson, "Low-Reynolds-number flow around a square cylinder at incidence: Study of blockage, onset of vortex shedding and outlet boundary condition," *Int. J. Numer. Methods Fluids*, vol. 26, no. 1, pp. 39–56, 1998, doi: 10.1002/(sici)1097-0363(19980115)26:1<39::aid-fld623>3.0.co;2-p.

[2] D. Biermann and W. H. Herrnstein, Jr, "The interference between struts in various combinations," *Natl. Advis. Comm. Aeronaut. Tech. Rep.*, vol. 468, no. 468, pp. 1–13, 1933.

[3] M. Grioni, S. A. Elaskar, and A. E. Mirasso, "A numerical study of the flow interference between two circular cylinders in tandem by scale-adaptive simulation model," *J. Appl. Fluid Mech.*, vol. 13, no. 1, pp. 169–183, 2020, doi: 10.29252/jafm.13.01.30185.

[4] M. R. Rastan and M. M. Alam, "Transition of wake flows past two circular or square cylinders in tandem," *Phys. Fluids*, vol. 33, no. 8, 2021, doi: 10.1063/5.0062978.

[5] W. Yang and M. A. Stremler, "Critical spacing of stationary tandem circular cylinders at Re≈100," *J. Fluids Struct.*, vol. 89, pp. 49–60, 2019, doi: 10.1016/j.jfluidstructs.2019.02.023.

[6] B. S. Carmo and J. R. Meneghini, "Numerical investigation of the flow around two circular cylinders in tandem," *J. Fluids Struct.*, vol. 22, no. 6–7, pp. 979–988, 2006, doi: 10.1016/j.jfluidstructs.2006.04.016.

[7] G. Schewe and M. Jacobs, "Experiments on the Flow around two tandem circular cylinders from sub- up to transcritical Reynolds numbers," *J. Fluids Struct.*, vol. 88, pp. 148–166, 2019, doi: 10.1016/j.jfluidstructs.2019.05.001.

[8] J. Wang, X. Shan, and J. Liu, "First instability of the flow past two tandem cylinders with different diameters," *Phys. Fluids*, vol. 34, no. 7, 2022, doi: 10.1063/5.0098204.

[9] M. M. Alam, "Lift forces induced by phase lag between the vortex sheddings from two tandem bluff bodies," *J. Fluids Struct.*, vol. 65, pp. 217–237, 2016, doi: 10.1016/j.jfluidstructs.2016.05.008.

[10] N. Mahír and Z. Altaç, "Numerical investigation of convective heat transfer in unsteady flow past two cylinders in tandem arrangements," *Int. J. Heat Fluid Flow*, vol. 29, no. 5, pp. 1309–1318, 2008, doi: 10.1016/j.ijheatfluidflow.2008.05.001.

[11] S. Singha and K. P. Sinhamahapatra, "High-Resolution numerical simulation of low reynolds number incompressible flow about two cylinders in tandem," *J. Fluids Eng. Trans. ASME*, vol. 132, no. 1, pp. 0111011–01110110, 2010, doi: 10.1115/1.4000649.